

Electrical conductivity, thermoelectric power, and ESR of a new family of molecular conductors, dicyanoquinonediimine-metal [(DCNQI)₂M] compounds

Takehiko Mori and Hiroo Inokuchi

Institute for Molecular Science, Myodaiji-cho, Okazaki-shi, Aichi 444, Japan

Akiko Kobayashi

Department of Chemistry, Faculty of Science, University of Tokyo, 7-3-1 Hongo, Bunkyo-ku, Tokyo 113, Japan

Reizo Kato and Hayao Kobayashi

Department of Chemistry, Faculty of Science, Toho University, Funabashi-shi, Chiba 274, Japan

(Received 19 January 1988)

A new family of organic molecules, 2- R_1 -5- R_2 -DCNQI (with $R_1, R_2 = \text{CH}_3, \text{CH}_3\text{O}, \text{Cl},$ or Br ; DCNQI = N, N' -dicyanoquinonediimine) works as a ligand as well as an electron acceptor to form highly conducting, charge-transfer and coordination compounds as (2- R_1 -5- R_2 -DCNQI)₂M (with $M = \text{Cu}, \text{Ag}, \text{Li}, \text{Na}, \text{K},$ or NH_4). These salts are investigated by the measurements of electrical conductivity, thermoelectric power, and electron spin resonance, which are appropriately understood by classifying them into three groups. Group-I DCNQI salts consisting of the salts with cations M other than Cu, undergo the Peierls transitions between 50 and 100 K. Their thermoelectric power is interpreted by the large- U limit of the Hubbard model. Group-II DCNQI salts, the Cu salts of the halogen-substituted DCNQI, also exhibit the Peierls transitions between 150 and 250 K, followed by the antiferromagnetic transitions around 10 K. With the one-dimensional tight-binding approximation, the bandwidth is estimated to be 0.4–0.5 eV. Group-III DCNQI salts, the Cu salts with $R_1 = R_2 = \text{CH}_3$ or CH_3O retain metallic conductivity down to 1.5 K, whereas a magnetic transition takes place at 5.5 K. This may be the first organic conductor in which metallic conduction and a magnetic order coexist. The magnetic order is attributed to the comparatively localized Cu^{2+} spins present independently of the conduction electrons on DCNQI, where the average oxidation state of Cu has been estimated to be $\text{Cu}^{1.3+}$.

In the history of organic conductors, the class of materials receiving most attention has often changed following the advance of the study. In the 1960's, a family of anion radical salts, TCNQ (7,7,8,8-tetracyanoquinodimethane) salts, were studied most intensively,¹ and since 1973, many studies have been devoted to complex salts such as TTF-TCNQ (TTF being tetrathiafulvalene). Since the discovery of the organic superconductor, much attention has been paid to the cation radical salts of TMTSF and BEDT-TTF [TMTSF, tetramethyl-tetraselenafulvalene; BEDT-TTF, bis(ethylenedithio)-tetrathiafulvalene],² though cation radical salts had been continuously studied since the first highly conducting charge-transfer complex perylene-Br.³ Apart from these organic charge-transfer complexes, highly conducting metal complexes such as KCP [$\text{K}_2\text{Pt}(\text{CN})_4\text{Br}_{0.3} \cdot 3\text{H}_2\text{O}$] have attracted continuous attention, and superconductivity has been found in the compounds of this category, (TTF)[Ni(mit)₂]₂ and [(CH₃)₄N][Ni(dmit)₂]₂ (dmit being isotrithionedithiolate).^{4,5}

Recently, Aumüller *et al.* have reported a new type of highly conducting molecular compound, (2,5-dimethyl-DCNQI)₂Cu.⁶ The molecule DCNQI is an acceptor with an analogous molecular structure to TCNQ, where the (NC)₂C= end groups of TCNQ are replaced by the

NCN= end groups (Fig. 1). Though DCNQI shows electron affinity comparable to that of TCNQ,⁷ and forms face-to-face stacks just like TCNQ in the charge-transfer complexes (Fig. 2), what is most characteristic of DCNQI is the coordination of the CN— end groups to the metal atoms; DCNQI works as a ligand as well as an electron acceptor. Thus the DCNQI complexes can be regarded as a new type of molecular conductors which are a combination of anion radical salts and metal complexes. Although the metal-metal distance (3.8 Å) is too long to realize high conductivity by the direct overlap of the metal orbitals, (2,5-dimethyl DCNQI)₂Cu shows quite high electrical conductivity ($> 10^3$ S/cm at room temperature) and retains metallic character down to (at least) 1.5 K.^{6,8} Moreover, the mixed valency of Cu ($\text{Cu}^{1.3+}$ on an average) has been indicated by x-ray photoelectron spectroscopy (XPS) and the $2k_F$ superlattice reflections of (2-methyl-5-chloro-DCNQI)₂Cu.⁸ Therefore, these Cu compounds possess two different types of unpaired electrons: itinerant electrons on DCNQI and localized electrons on Cu^{2+} .

In order to investigate this series of compounds, the authors have prepared various acceptors by changing the substituents R_1 and R_2 as shown in Fig. 1, and obtained their complexes represented as (2- R_1 -5- R_2 -DCNQI)₂M

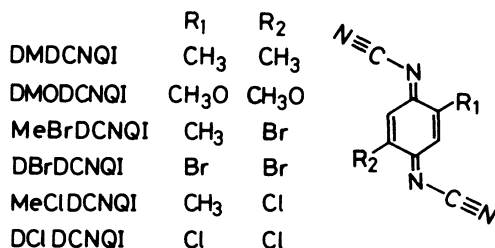


FIG. 1. The molecular structures and their abbreviations of the DCNQI series molecules investigated in the present work.

with various cations, $M = \text{Cu, Ag, Li, Na, K, and NH}_4$.⁹ Low-temperature x-ray investigation, x-ray photoelectron spectroscopy, energy-band calculation, and the pressure-induced metal-insulator transition of (2,5-dimethyl-DCNQI)₂Cu have been reported elsewhere.^{8,10} In the present paper, the authors report the systematic study of electrical conductivity, thermoelectric power (Seebeck effect), and electron spin resonance, for a fundamental understanding of the physical properties of these new types of compounds.

II. EXPERIMENT

The measurements of the electrical resistivity, the thermoelectric power, and ESR were performed between liquid-helium and room temperatures. These complexes investigated are essentially isostructural, belonging to a tetragonal system (Fig. 2),¹¹ where the c axis is parallel to the stack of the DCNQI.^{8,9} Because the samples were thin needle, all measurements of the electrical resistivity and the thermoelectric power were carried out along the needle direction (c axis).

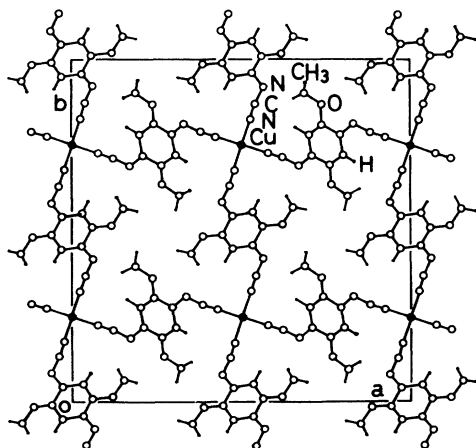


FIG. 2. Crystal structure of (2,5-dimethoxy-DCNQI)₂Cu, projection along the tetragonal c axis.

The electrical resistivity was measured by the conventional four-probe method with low-frequency (80-Hz) alternating current. The electrical contacts were made with gold paint.

The thermoelectric power was measured by attaching a sample to two copper heat blocks with carbon paint. The heat blocks are alternately heated (for 2 min above liquid-nitrogen temperature and for 5 sec at liquid-helium temperature) to generate a temperature gradient (of about 0.5 K between 100 and 300 K and about 0.2 K at 4 K). The generated electromotive forces of the sample and of the differential thermocouple (for the measurement of the temperature difference) were processed on a microcomputer, which, in turn, controlled the heating of the blocks.

The ESR spectra were measured with a conventional Varian Associates X-band E112 spectrometer. The temperature control was achieved using an Oxford Instruments ESR9 continuous-flow helium cryostat. The samples were mounted on a Teflon holder in a 4-mm-diam quartz ESR tube with 10-Torr He exchange gas. Most measurements were carried out by using a single crystal, though a bundle of very thin crystals was used in several cases. Since all observed spectra were symmetrical Lorentzian, the intensity was estimated from the peak-to-peak linewidth and the amplitude. In several cases, the numerical double integration of the digitized data was used together.

III. ELECTRICAL CONDUCTIVITY

All samples reported here showed metallic conductivity at room temperature. The results of the conductivity measurements are summarized in Table I. The samples can be classified in three groups according to the temperature dependence of the conductivity.

Group I includes all samples having cations other than Cu. The room-temperature conductivities of this group are around 100 S/cm, except about 300 S/cm of the Li salts. The temperature dependence of the resistivity is shown in Fig. 3. These samples undergo metal-insulator transitions at $T_{M-I} = 50\text{--}200$ K. As shown in curves b and d of Fig. 3, some samples show very large hysteresis; the steep rise of the resistivity differs by as much as 80 K in cooling and heating. In addition, these samples tend to show resistance jumps around T_{M-I} . Such a behavior has been observed in, for example, (TTF) X_x ($X = \text{I, SCN, etc.}$),^{12,13} which are highly one-dimensional conductors. The DCNQI salts are also considered to be highly anisotropic, because the path of the conduction electrons is strictly limited to the stack of the DCNQI molecules due to the poor electron affinity of the counter cations. The conduction of these highly one-dimensional systems may be easily affected by the activated hopping between microdomains, and tend to show jumps with the development of the microdomains. The microdomains might grow under the influence of some intrinsic structural change such as the Peierls distortion, which is, as will be discussed later, the inherent origin of the metal-insulator transition. Therefore, the resistance rises at the cooling

TABLE I. Room-temperature conductivity, metal-insulator transition temperature, and energy gap observed in the conductivity measurements.

Compound	σ_{rt} (S/cm)	T_{M-I} (K)	E_a (eV)
Group I			
(2,5-dimethyl-DCNQI) ₂ Ag	100	100	0.1
(2-methyl-5-chloro-DCNQI) ₂ Ag	80	90	0.03
(2,5-dimethyl-DCNQI) ₂ Li	300	80	0.02
(2-methyl-5-chloro-DCNQI) ₂ Li	300	70	0.02
(2,5-dimethoxy-DCNQI) ₂ Li	200	100	0.02
(2,5-dimethyl-DCNQI) ₂ Na	100	150	0.05–0.1
(2,5-dimethoxy-DCNQI) ₂ Na	100	120	0.03
(2,5-dimethyl-DCNQI) ₂ K	70	180	0.03
(2,5-dimethyl-DCNQI) ₂ NH ₄	60	130	0.04
(2-methyl-5-chloro-DCNQI) ₂ NH ₄	70	140	0.06
Group II			
(2-methyl-5-bromo-DCNQI) ₂ Cu	700	160	0.045 ^a
(2,5-dibromo-DCNQI) ₂ Cu	700	180	0.045 ^a
(2-methyl-5-chloro-DCNQI) ₂ Cu	700	210	0.045
(2,5-dichloro-DCNQI) ₂ Cu	700	235	0.045 ^a
Group III			
(2,5-dimethyl-DCNQI) ₂ Cu	1000–2000	Metallic down to 1.5 K	
(2,5-dimethoxy-DCNQI) ₂ Cu	700	Metallic down to 1.5 K	

^a The values around 100 K; 0.02 eV below 50 K.

run, which should be regarded as closer to the inherent transitions, are listed in Table I.¹⁴ The transition temperatures are almost common to the same counter cation, and not much affected by the change of the substituents of the DCNQI.

When the resistivity is plotted in $\log \rho$ versus $1/T$, around T_{M-I} the energy gap develops rapidly in some compounds, but develops gradually in others. Because in both cases the energy gap approaches a constant value at sufficiently lower temperatures than T_{M-I} , the activation

energies are extracted in this low-temperature region (around 50 K) as listed in Table I. These values are reasonable in comparison with T_c .

The Cu salts of the halogen-substituted DCNQI constitute the second group. These salts show intermediately high conductivity, 700 S/cm, at room temperature (Table I), and undergo metal-insulator transitions at relatively high temperatures (Fig. 4). The activation energies of the semiconducting region are almost the same for these four salts: 0.045 eV around 100 K and 0.02 eV below 50 K. There is a steep rise of the resistivity at T_{M-I} , indicating the rapid formation of the energy gap. The magnitude of the steep rise decreases in the order of 2-methyl-5-bromo-DCNQI, 2,5-dibromo-DCNQI, 2-methyl-5-

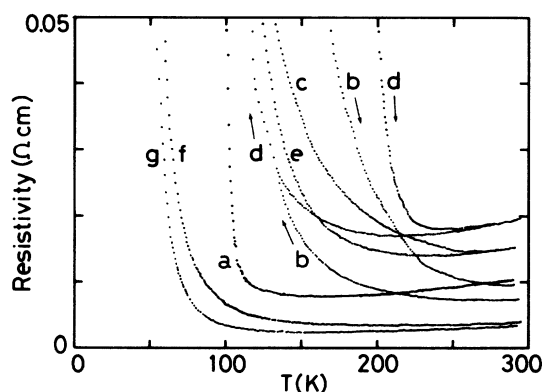


FIG. 3. Electrical resistivity of group-I DCNQI salts; curve a: (2,5-dimethyl-DCNQI)₂Ag, curve b: (2,5-dimethyl-DCNQI)₂Na, curve c: (2,5-dimethyl-DCNQI)₂K, curve d: (2,5-dimethyl-DCNQI)₂NH₄, curve e: (2-methyl-5-chloro-DCNQI)₂NH₄, curve f: (2,5-dimethyl-DCNQI)₂Li, and curve g: (2-methyl-5-chloro-DCNQI)₂Li. For samples b and d, the hystereses are shown.

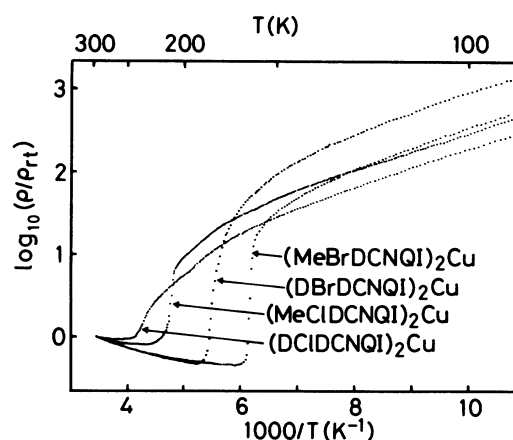


FIG. 4. Normalized electrical resistivity of the group-II DCNQI salts, Arrhenius plots.

chloro-DCNQI, and 2,5-dichloro-DCNQI, whereas T_{M-I} increases in this order. This order corresponds to the order of the electron affinity of the substituents.

The members of group III are the Cu salts of 2,5-dimethyl-DCNQI and 2,5-dimethoxy-DCNQI. In addition to (2,5-dimethyl-DCNQI)₂Cu, first reported by Aumüller *et al.*⁶ the authors found the methoxy analog, (2,5-dimethoxy-DCNQI)₂Cu, to show similar metallic behavior (Fig. 5).¹⁵ Though the room-temperature conductivity, 700 S/cm, of the latter is somewhat lower (Table I), this might be due to the poorer quality of the latter crystals. These salts show $\rho \propto T^{2.3}$ dependence above 30 K; this large temperature dependence implies some mechanism enhancing the electron scattering, which has attracted much attention to the high conductivity of the quasi-one-dimensional conductors such as TTF-TCNQ and (SN)_x.¹⁶ The resistivity becomes constant below 30 K. This low-temperature conductivity is as high as $> 10^5$ S/cm, which is one of the highest values of molecular conductors.

Contrary to the salts of the other cations, the Cu salts are sensitive to the change of the substituents. If the substituents are electron-donating moieties such as methyl and methoxy (group III), the metal-insulator transition does not take place. On the contrary, if the electron-withdrawing moieties such as halogen are included (group II), the metal-insulator transition occurs and T_{M-I} rises with increasing the electron affinity of the substituents. Because the $2k_F$ satellite reflections have been found in the low-temperature x-ray investigation of (2-methyl-5-chloro-DCNQI)₂Cu,⁸ these transitions can be considered as the Peierls type. The enhancement of the electron affinity of the substituents makes the molecule a better acceptor, and may increase the charge transfer to change $2k_F$. If the resulting $2k_F$ approached a commensurate value, the transition temperature would increase by "locking in" that value (probably $c^*/3$). The charge transfer determined by XPS, however, showed no significant difference between (2-methyl-5-chloro-

DCNQI)₂Cu and (2,5-dimethyl-DCNQI)₂Cu.⁸

The x-ray structure analysis indicates that the enhancement of the electron affinity of the acceptor shortens the Cu-N distance, strengthening the ligand field to increase the Jahn-Teller distortion around Cu.¹⁵ It has been pointed out that the splitting of the *d* levels associated with the ligand-field distortion reduced the hybridization of the Cu orbitals with the DCNQI conduction orbitals. Then the interchain coupling decreases to result in the increase of T_{M-I} (as far as the mean field approach is valid). From the viewpoint of the band structure, the reduction of T_{M-I} has been interpreted by a "multi-Fermi-surface" situation derived from the hybridization of the Cu orbitals.⁸ Though the lock-in mechanism cannot be entirely ruled out, the authors consider the hybridization of the Cu *d* orbitals with the DCNQI conduction orbitals to be important. Anyway, the subtle change of T_{M-I} that is characteristic of the Cu salts is closely related to the mixed valency of Cu.

IV. THERMOELECTRIC POWER

The thermoelectric power of the group-I DCNQI salts is shown in Fig. 6. These salts show a constant thermoelectric power, around $-60 \mu\text{V/K}$ at high temperatures, and undergo metal-insulator transitions between 50 and 100 K.

The constant high-temperature thermoelectric power of the magnitude of $-60 \mu\text{V/K}$ has been observed in many TCNQ salts.¹⁷ The thermoelectric power based on the large-*U* limit of the Hubbard model is obtained as¹⁸

$$S = -\frac{k_B}{e} \ln \left[\frac{2(1-\rho)}{\rho} \right]. \quad (1)$$

Since the band-filling parameter of the present 2:1 salts is

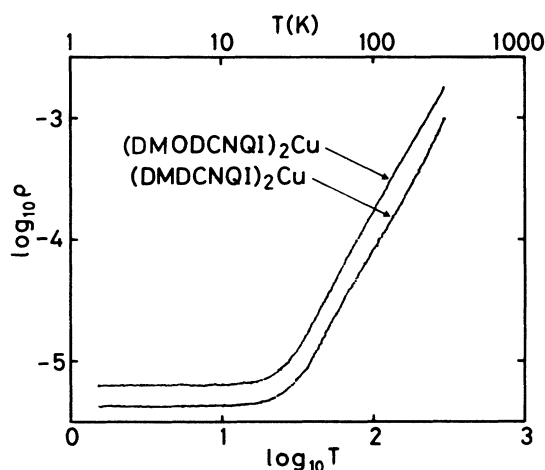


FIG. 5. Electrical resistivity of the group-III DCNQI salts. Both the horizontal and the vertical axes are plotted logarithmically.

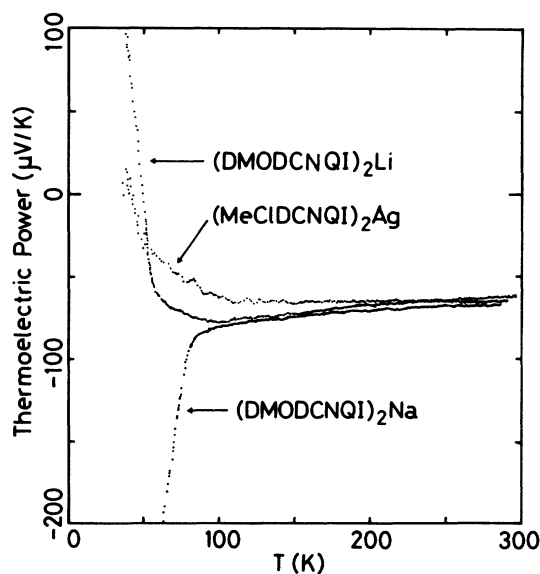


FIG. 6. Thermoelectric power of the group-I DCNQI salts. The small contribution of the copper counter-electrodes has not been subtracted.

$\rho = \frac{1}{2}$, the above equation leads to $S = -(k_B/e) \ln 2 = -58.9 \mu\text{V}/\text{K}$. The factor $\ln 2$ can be regarded as the entropy of the N electrons to put on singly occupiable $2N$ sites.¹⁹ The universally observed constant thermoelectric power indicates the importance of the Coulomb repulsion in the present system.

The metal-insulator transition temperatures observed in the thermoelectric power are considerably lower than those of the conductivities (compare Fig. 6 and Table I). Because thermoelectric power is a zero-current transport property, it is not limited by sample imperfections, as long as most temperature gradient is applied across the unbroken regions. Thus, thermoelectric power is generally less affected by the crystal imperfections and the microdomains. As discussed in the last section, the conductivity of the group-I DCNQI salts is largely affected by the development of microdomains. The results of the thermoelectric power indicate that the intrinsic T_{M-I} is considerably lower than the rises of the resistivity; the inherent T_{M-I} is between 50 and 100 K. This will be confirmed later by the ESR measurements.

The activation energies of the thermoelectric power obtained around 50 K are 0.017 and 0.03 eV for (2,5-dimethoxy-DCNQI)₂Li and (2,5-dimethoxy-DCNQI)₂Na, respectively. These values agree with the activation energies of the resistivity (Table I) evaluated in the same temperature region.

The thermoelectric power of the group-II DCNQI salts is depicted in Fig. 7. Above T_{M-I} , the thermoelectric power is approximately proportional to T , that is, the typical behavior of metals. Assuming the one-dimensional tight-binding band, the thermoelectric power is,²⁰

$$S = -\frac{\pi^2 k_B^2 T}{6et} \frac{\cos(\frac{1}{2}\pi\rho)}{1 - \cos^2(\frac{1}{2}\pi\rho)} \quad (2)$$

where t is the transfer integral. The band-filling parameter $\rho = \frac{2}{3}$ has been estimated from the x-ray photoelectron spectra and the $2k_F$ satellites.⁸ Then the room-temperature value, 20–25 $\mu\text{V}/\text{K}$, or equivalently the

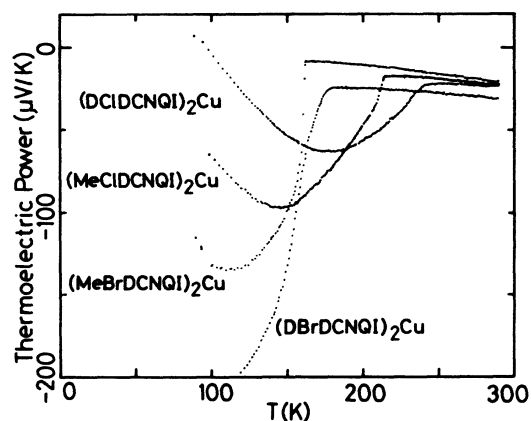


FIG. 7. Thermoelectric power of the group-II DCNQI salts.

slope, 0.06–0.08 $\mu\text{V}/\text{K}^2$ offers the bandwidth, $4t = 0.4\text{--}0.5$ eV. This value is almost the same as those of the TCNQ salts,²¹ as would be expected from the similarity of the molecular structure and the molecular packing.^{1,8}

Although the molecular stack of the DCNQI and, as a consequence, probably also the bandwidths are not largely different in the group-I and group-II DCNQI salts, the thermoelectric power is appropriately interpreted by the large- U Hubbard model for the group-I DCNQI salts, and by the band model for the group-II DCNQI salts. This fact indicates that the reduction of effective U takes place in the Cu-containing salts. This may be due to the larger extension of the DCNQI conduction orbitals to the Cu sites; the hybridization of the mixed-valence Cu orbitals plays an important role in the reduction of the effective Coulomb repulsion as well as the enhancement of the interchain interaction.

The transition temperatures observed in Fig. 7 correspond with the results of the conductivity (Table I), indicating the effect of the imperfections is not significant in the group-II DCNQI salts. Just below T_{M-I} , the absolute value of the thermoelectric power rapidly increases, especially in the Br-containing salts, due to the rapid formation of the energy gap. With decreasing temperature, the thermoelectric power makes a minimum, and increases again following the $1/T$ relation. In (2,5-dichloro-DCNQI)₂Cu, the sign becomes positive below 100 K. The $1/T$ dependence of the Cl-containing salts below the minimum gives the activation energy of 0.02 eV. This value agrees with the low-temperature activation energy of the conductivity. In this semiconducting region, the thermopower is determined by the relative mobilities of the electrons and holes which are generated below and above the energy gap. Then the sign of the thermoelectric power is determined by the small detail of the band structure around E_F . The same discussion is also valid for the semiconducting region of the group-I DCNQI salts; the results of Fig. 6 designate no systematic rule whether the thermoelectric power rises in the positive or negative directions.

The thermoelectric power of the group-III DCNQI salts is not simply metallic (Fig. 8). The temperature dependence of the thermoelectric power is almost the same for these two compounds. There is a peak between 50 and 60 K; this kind of peak has sometimes been observed in highly conducting materials.²² A possible origin of this peak is phonon drag.²³ In that case, below the peak, the thermoelectric power should go to zero following a T^3 behavior. This dependence is actually observed in (2,5-dimethoxy-DCNQI)₂Cu, whereas the temperature dependence of (2,5-dimethyl-DCNQI)₂Cu follows a linear T behavior.

Another problem is the relatively large absolute value of the thermoelectric power, that is $-34 \mu\text{V}/\text{K}$ at room temperature. This value is intermediate between those of the group-I and group-II DCNQI salts, and gives an anomalously small bandwidth by a simple application of Eq. (2). However, assuming some constant enhancement added to Eq. (1), the slope, 0.05–0.06 $\mu\text{V}/\text{K}^2$ at 200–300 K offers the bandwidth, 0.5–0.65 eV. Anyway, the tem-

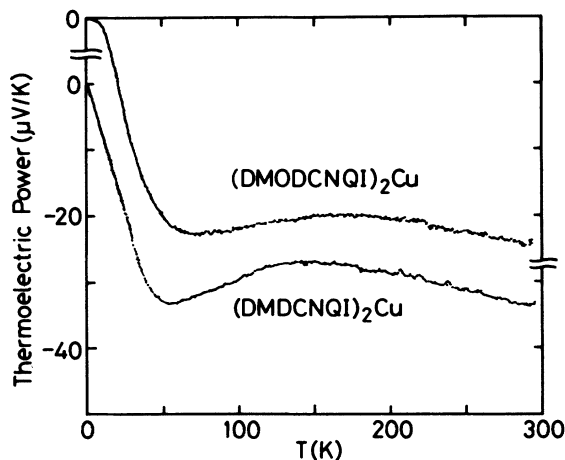


FIG. 8. Thermoelectric power of the group-III DCNQI salts.

perature dependence suggests that the simple one-dimensional energy-band picture which seems to be valid for the group-II DCNQI salts is not applicable to this group. This is probably due to the large hybridization of the DCNQI and the Cu orbitals, and the resulting complicated band structure.⁸

V. ELECTRON SPIN RESONANCE

Because the crystal belongs to a tetragonal system, the g tensor has uniaxial symmetry. The principal g values which are properly fitted to the relation

$$g^2 = g_c^2 \sin^2 \theta + g_a^2 \cos^2 \theta \quad (3)$$

by using the data of the angular dependence are listed in Table II. For the group-I DCNQI salts, the g values are almost independent of the compounds; those are regarded

as characteristic of the DCNQI molecule. The larger shift from the free-electron value is observed in the a direction. Because the molecular plane is approximately perpendicular to the c axis, this anisotropy indicates the π character of the unpaired electron. Since the DCNQI molecules are, unfortunately, not parallel to each other, these values are not quantitatively related to the molecular orbitals.

The magnitude of the g shift is comparable to TCNQ: $g_1 = 2.0032$, $g_2 = 2.0026$, and $g_3 = 2.0024$.²⁴ The ESR spectra of many anion radical salts of TCNQ, however, show fine structures due to their comparatively low electron conduction. Like the metallic complex salts of TCNQ such as TTF-TCNQ, the present salts give single Lorentzians due to the motional narrowing. The sharp linewidth < 1 G at room temperature (Table II) is comparable to 0.4 G of the relatively high-conductive quinolinium-TCNQ.²⁴ Such a small linewidth is a result of the one dimensionality of the conduction electrons, because in a one-dimensional metal the scattering of electrons by phonons is limited to those (1) from near k_F to k_F and (2) from near $-k_F$ to k_F .²⁵ Both of these scatterings contribute little to spin flip to give rise to the large relaxation time in comparison with the prediction of the Elliott mechanism of three dimensions ($\Delta H > 100$ G).²⁶

As shown in Table II and Fig. 9, the Ag-containing salts show slightly large g shifts (> 2.004) and large linewidths (around 17 G). This is due to the large spin-orbit coupling of Ag, and indicates a small interaction of the Ag orbital and the DCNQI orbitals. The linewidth of (2-methyl-5-chloro-DCNQI)₂Ag is largest along $H_0 \parallel a$ (Fig. 9), namely the direction of the largest g shift, though the anisotropic fraction is only 11% of the total linewidth. In the alkali-metal complexes the anisotropy of the linewidth is very small (Table II).

The g values of the group-I salts show no temperature dependence. With decreasing the temperature, the linewidth decreases following the temperature depen-

TABLE II. Principal g values, peak-to-peak linewidths at room temperature, and activation energies of Eq. (4) obtained from the ESR investigation.

Compound	g_c	g_a	ΔH_c (G)	ΔH_a (G)	E_a (eV)
Group I					
(2,5-dimethyl-DCNQI) ₂ Ag		2.0041		16.5	0.016
(2-methyl-5-chloro-DCNQI) ₂ Ag	2.0018	2.0046	16	18	0.016
(30 K)	2.0023	2.0056	8	9	
(2,5-dimethyl-DCNQI) ₂ Li		2.0036		0.7	0.011
(2-methyl-5-chloro-DCNQI) ₂ Li		2.0035		0.61	0.009
(2,5-dimethoxy-DCNQI) ₂ Li	2.0020	2.0035	0.3	0.32	0.012
(30 K)	2.0020	2.0035	0.27	0.24	
(2,5-dimethyl-DCNQI) ₂ K	2.0019	2.0032	0.46	0.43	0.011
(2,5-dimethoxy-DCNQI) ₂ Na	2.0019	2.0038	0.19	0.18	0.019
Group II ^a					
(2-methyl-5-bromo-DCNQI) ₂ Cu	2.388	2.070	170	165	
(2,5-dibromo-DCNQI) ₂ Cu		2.060		135	
(2-methyl-5-chloro-DCNQI) ₂ Cu		2.076		63	
Group III ^a					
(2,5-dimethyl-DCNQI) ₂ Cu	2.408	2.079		23	

^a The values at 30 K.

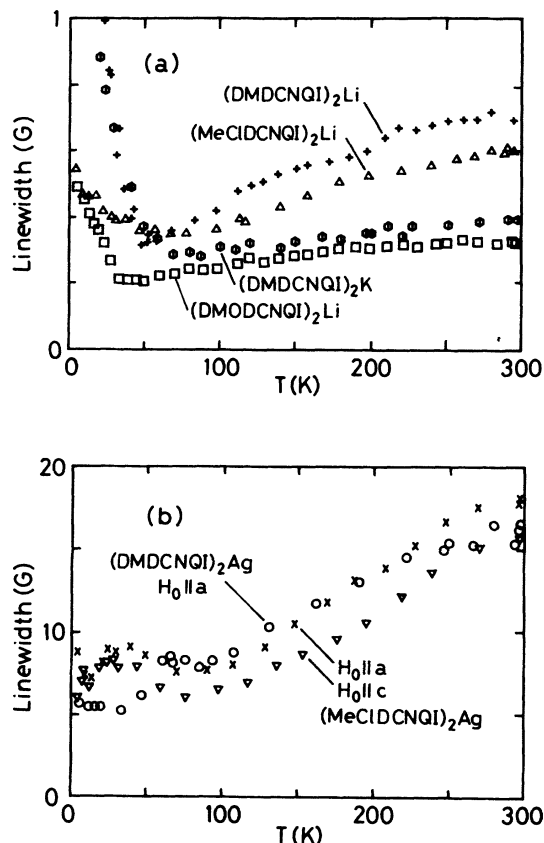


FIG. 9. Temperature dependence of the ESR peak-to-peak linewidth, (a) the alkali-metal salts, and (b) the Ag salts.

dence, $\Delta H = A + BT$ as shown in Fig. 9. The increase of the linewidth below T_{M-I} is not due to intrinsic origin.

The temperature dependence of the ESR intensity is shown in Fig. 10. The intensity is almost constant or weakly temperature dependent at high temperatures, and falls to zero around 50 K. The low-temperature behavior follows the activated process,

$$I = \frac{2C}{k_B T} \left[3 + \exp \left(\frac{E_a}{k_B T} \right) \right]^{-1} \quad (4)$$

where the activation energies E_a are listed in Table II. The energy gaps 0.01–0.02 eV are the same order as the activation energies of the conductivity (Table I). These results strongly indicate the universal occurrence of the Peierls transitions at $T_{M-I} = 50$ –100 K and with the energy gap of the order of 0.02 eV. In some samples in Fig. 10, decrease of the intensity occurs at considerably higher temperature than T_{M-I} . This suggests the decrease of the states density due to the fluctuation of the Peierls distortion.

In the case of the Cu-containing DCNQI salts (groups II and III), ESR signal is not observed at room temperature. A comparatively broad single Lorentzian appears below about 80 K. The g values [$g_c = 2.388$, $g_a = 2.070$ for (2-methyl-5-bromo-DCNQI)₂Cu at 30 K] show a large shift from the free-electron value in comparison with the

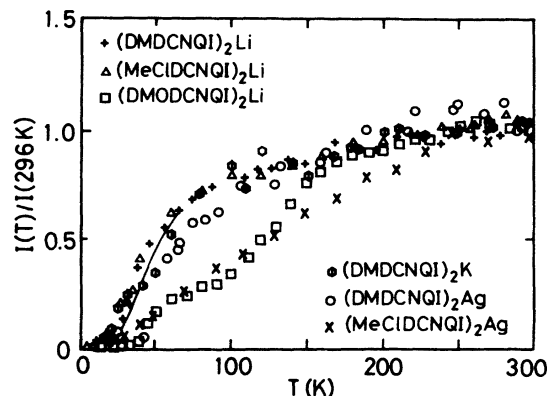


FIG. 10. Temperature dependence of the ESR intensity for the group-I salts, normalized by the room-temperature value. The small Curie-like contribution due to impurities has been subtracted. The solid curve represents the temperature dependence of Eq. (4) with $E_a = 0.02$ eV.

group-I DCNQI salts. These g values are, however, typical values of the Cu^{2+} ions.²⁷ The large linewidths are also attributable to the large spin-orbit coupling of the Cu ions. In addition, the Peierls gap at the conduction band of the DCNQI is developed in this semiconducting temperature region of the group-II DCNQI salts. Therefore, the spins observed by ESR are considered to be located on the Cu ions.

The anisotropic g shift of the local spins on transition elements is predicted from the crystal-field theory.²⁷ In the present compounds, the Cu atoms are coordinated in a tetrahedral shape shortened along the c direction.⁸ The tetrahedral crystal field splits the d levels into E_g (Γ_3) and T_{2g} (Γ_5) levels (Fig. 11). In the $\text{Cu}^{2+}(d^9)$ system, one hole is present on the T_{2g} level. The tetragonal distortion further splits the T_{2g} levels to the B_2 singlet and the E doublet according to its D_{2d} point-group symmetry. By considering this tetragonal distortion and the spin-orbit coupling at the same time, and neglecting the admixture of the E_g levels, the g value of the ground state becomes²⁸

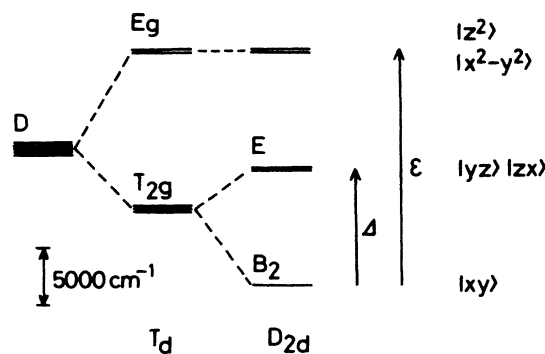


FIG. 11. Schematic representation of the splitting of a D state in a tetrahedral field with a tetragonal (D_{2d}) distortion, including no spin-orbit coupling. The level separations are taken from the model calculation.

$$\begin{aligned}
 g_c &= -1 - 3 \cos(2\delta), \\
 g_a &= |1 - \cos(2\delta) + \sqrt{2} \sin(2\delta)|, \\
 \tan(2\delta) &= \frac{\sqrt{2}\lambda}{\Delta + \frac{1}{2}\lambda}, \quad 0 < \delta < \frac{\pi}{2}
 \end{aligned}
 \quad (5)$$

where λ is the spin-orbit parameter ($\lambda < 0$), and $\Delta = E(E) - E(B_2)$ is the crystal-field energy by the tetragonal distortion. The difference of g from the free-electron value becomes extraordinarily large for electrons in states near a degeneracy. For example, if the E doublet is the ground state ($\Delta/\delta \rightarrow \infty$ and $\delta=0$), Eq. (5) yields $g_c = -4$ and $g_a = 0$. This possibility is evidently excluded by the observed g values.

In order to roughly estimate the splitting of the d levels, the authors carried out a model calculation.²⁹ The results are $\epsilon = E(E_g) - E(B_2) = 19000 \text{ cm}^{-1}$ and $\Delta = 9000 \text{ cm}^{-1}$; the ground state is B_2 (Fig. 11). When the B_2 level is the ground state, the spin only value $g_c = g_a = 2$ is realized in Eq. (5) ($\delta = \pi/2$). Because in Eq. (5), g_c and g_a never become > 2 at the same time, the observed g shift should be attributed to the contribution of the E_g levels. Such a g shift is given to first order,

$$\Delta g = -2\lambda \sum_n \frac{\langle g | L | n \rangle \langle n | L | g \rangle}{E_n - E_g}. \quad (6)$$

Since the wave function (one of the Kramers doublet) of the level of Eq. (5) is³⁰

$$A^+ = \cos\delta | +1^- \rangle - \sin\delta | 0^+ \rangle, \quad (7)$$

the g shift is³¹

$$\Delta g_c = -\frac{8\lambda'}{\epsilon} \sin^2\delta, \quad \Delta g_a = -\frac{4\lambda'}{\epsilon} \cos^2\delta. \quad (8)$$

Because now $\delta \sim \pi/2$, Δg_c almost entirely comes from ϵ , whereas Δg_a comes from Δ [from Eq. (5)]. By combining Eq. (8) with Eq. (5), the observed g shifts give $\epsilon = -20\lambda'$ and $\Delta = -29\lambda'$.³² Though these values are, if the free-atom value $\lambda = -830 \text{ cm}^{-1}$ is used, of correct order in comparison with the estimation by the molecular-orbital calculation, the relation $\epsilon < \Delta$ conflicts with the first starting point. This unphysical result suggests that the crystal-field approximation is not appropriate for the present system due to the considerable mixing of the ligand orbitals to the d orbitals. By taking into account the hybridization, the above result should be read as³³

$$\epsilon = -20k^2\lambda, \quad \Delta = -29(k')^2\lambda \quad (9)$$

with the orbital reduction factors k for the E_g orbitals, and k' for the T_{2g} orbitals ($k, k' \leq 1$). Compared with the model calculation, ϵ is directly of correct order, namely $k \approx 1$, whereas Δ gives rise to $k' = 0.625$. This means that the covalency is significant for the T_{2g} orbitals, but insignificant for the E_g orbitals. This result is reasonable in view of the geometry of the molecular orbitals. The similar tendency has been observed in other tetrahedrally coordinated Cu^{2+} .³⁴

It should be noted that the squashed tetrahedron of the present complex can be regarded as a coordination inter-

mediate between a tetrahedron and a square plane. In a square planar Cu^{2+} complex, the g value anisotropy that is essentially similar to the present complex has been observed; $g_c = 2.266$ and $g_a = 2.053$ for an acetylaceton complex.³⁵

When the T_{2g} levels are nearly degenerate, Eq. (5) offers another solution. At $\Delta=0$, Eq. (5) yields $g_c = -2$ and $g_a = 2$. By assuming the contribution of the E_g levels to be approximated by Eq. (8), the combination of Eqs. (5) and (8) satisfies the observed g values at $\epsilon = 5900 \text{ cm}^{-1}$ and $\Delta = -350 \text{ cm}^{-1}$. This ϵ is, however, too small compared with the model calculation.

The g values show no temperature dependence. The temperature dependence of the linewidth is depicted in Fig. 12. The linewidth is almost constant up to about 30 K, then gradually broadens with increasing temperature. Though the behavior of the temperature dependence seems to be common in the three salts in Fig. 12, the magnitude of the linewidth is quite different; the substituents, Cl and Br, considerably broaden the linewidth. This suggests the linewidth is influenced by the spin-orbit coupling of the substituents due to a finite spread of the observed spin to the DCNQI molecules.

As shown in Fig. 13, the ESR intensity of the group-II salts varies following the Curie-Weiss relation:

$$I = \frac{C}{T - \Theta}. \quad (10)$$

The Weiss temperatures, Θ are listed in Table III. At a low temperature T_N , the ESR signal suddenly broadens and seems to disappear. Because Θ is negative, it is quite natural to consider this transition as an antiferromagnetic spin order. In the three-dimensional Ising or Heisenberg antiferromagnet, $|T_N/\Theta|$ should be 0.6–0.8.³⁶ Though T_N (Néel temperature) in Table III is not sufficiently accurate due to the difficulty of temperature control in this temperature region, the observed values roughly satisfy the theoretical prediction. The magnitude of the Curie constant is consistent with the spin concentration deduced from $\text{Cu}^{1.3+}$, where $S = \frac{1}{2}$ spins exist on $\frac{1}{3}$ of the Cu sites.

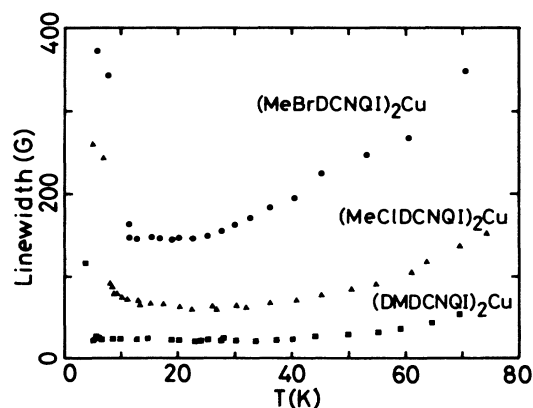


FIG. 12. Temperature dependence of the peak-to-peak linewidth for the group-II and group-III DCNQI salts.

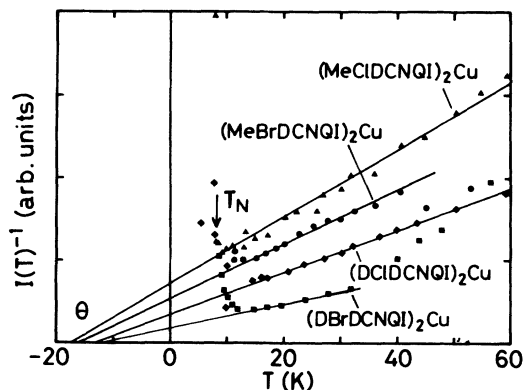


FIG. 13. Temperature dependence of the inverse ESR intensity for the group-II DCNQI salts.

The absence of the ESR signal at room temperature is due to the broadening of the linewidth and decreasing Curie-Weiss temperature dependence of the intensity. As a general tendency, the ESR signal of d^9 (Cu^{2+}) is observable only at very low temperatures (typically < 30 K), especially in the case of high symmetry, because the incomplete quenching of the orbital angular momentum considerably shortens the relaxation time.^{34,37} The signal can be observed at room temperature only in the compounds with obviously low symmetry.^{35,38}

A similar discussion is also valid for (2,5-dimethyl-DCNQI)₂Cu. The signal of (2,5-dimethyl-DCNQI)₂Cu is observed only below 70 K. The narrower linewidth than the group-II DCNQI salts (Fig. 12) can be attributed to, besides the smaller spin-orbit coupling of the substituents, the exchange interaction with the conduction electrons. However, similarity in the g value to the group-II DCNQI salts (Table II) indicates that the observed signal also comes from the spins on Cu^{2+} . Since, in addition, the g value and the linewidth show no temperature dependence, it is not necessary to consider an anomalous coupling of the localized spin and the conduction electrons.³⁹ The ESR signal of the related salt, (2,5-dimethoxy-DCNQI)₂Cu, was unfortunately not observed, probably due to the smallness of the crystals.

As shown in Fig. 14, the ESR intensity of (2,5-dimethyl-DCNQI)₂Cu increases rather rapidly below 60 K. The intensity makes a broad maximum at 30 K, decreases again, and the ESR signal suddenly broadens to vanish at 5.5 K. Since the disappearance of the signal

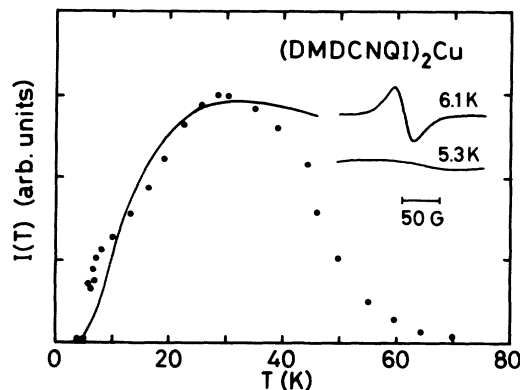


FIG. 14. Temperature dependence of the ESR intensity of (2,5-dimethyl-DCNQI)₂Cu. The solid line represents the prediction of the singlet-triplet model [Eq. (4)].

closely resembles the group-II DCNQI salts, it is highly possible that some kind of magnetic order takes place at this temperature. The considerable decrease of the intensity between 30 and 5.5 K may be due to the development of a short-range magnetic order. Since the present compounds are highly anisotropic, the existence of such a large fluctuation is reasonable. Therefore, (2,5-dimethyl-DCNQI)₂Cu has two characteristic temperatures: the onset of short-range one-dimensional order at 30 K related to the intrachain exchange interaction, and the long-range three-dimensional transition at 5.5 K associated with the interchain interaction. The difference of the group-II and group-III DCNQI salts may arise from the existence of the conduction electrons in this temperature region.

Since the linewidth between 5.5 and 60 K shows very small temperature dependence, the ESR intensity can be estimated with reasonable accuracy to allow a little more quantitative discussion. The intensity shown in Fig. 14 is, however, not fitted to the prediction of any simple magnetic model systems such as the one-dimensional (or two-dimensional) Heisenberg (or Ising) systems.³⁶ These models lead to much weaker temperature dependence than the observation. Figure 14 shows a prediction of the singlet-triplet model represented by Eq. (4) ($2J/k_B = E_a/k_B = 21$ K), where the Cu^{2+} spins are expected to be dimerized. Though the agreement is not quite good, the low-temperature behavior has some possibility to be approximately explained by this kind of model. However, it seems to be very difficult to reproduce the strong temperature dependence above 30 K. It is desirable that static susceptibility or heat capacity will be measured to be compared with a theoretical model.

At high temperatures, the Cu^{2+} is regarded as randomly distributed. Therefore, a question arises as to which temperature, if any, orders the Cu^{2+} . If the magnetic order takes place prior to the order of Cu^{2+} , one can imagine a situation like a spin-glass state. The authors, however, temporarily suppose that the magnetic order is accompanied by the order of Cu^{2+} : a short-range order at 30 K and a long-range order at 5.5 K. In this case, the

TABLE III. Néel temperature T_N and Weiss temperature Θ determined by the ESR experiments.

Compound	T_N (K)	Θ (K)
(2-methyl-5-bromo-DCNQI) ₂ Cu	11	-16
(2,5-dibromo-DCNQI) ₂ Cu	13	-12
(2-methyl-5-chloro-DCNQI) ₂ Cu	8	-17
(2,5-dichloro-DCNQI) ₂ Cu	10	-13
(2,5-dimethyl-DCNQI) ₂ Cu	(5.5)	

model of the spin system has to include the freedom of the Cu^{2+} sites as well as the orientation of the spins. This seems to be quite consistent with the above dimerization model. Though the microscopic feature is still unclear, the present system may be the first organic system where the metallic electron and the ordered spins are coexisting.

At 5.5 K the conductivity (Fig. 5) and the thermoelectric power show nothing anomalous. When a magnetic order is developed in the Cu sites, a finite fluctuation of the spin density is expected to be induced on the DCNQI chains. On the other hand, organic conductors are generally very sensitive to the instability of spin-density waves. For example, the spin-density waves on a small fraction (10–20 %) of the electrons makes $(\text{TMTSF})_2\text{X}$ insulating.⁴⁰ Therefore, it is surprising that the magnetic order of the Cu^{2+} spins produces no influence on the conduction electrons of the DCNQI molecules. Moreover, if the dimerization of the Cu^{2+} spins takes place, it is highly possible that the magnetic order is accompanied by a kind of charge-density wave on the Cu^{2+} sites. In the case of the *f*-band metals, the anomaly of the resistivity at T_N is small; only the temperature gradient changes at T_N .⁴¹ Since (2,5-dimethyl-DCNQI)₂Cu shows residual resistivity in the temperature region of T_N , the lack of anomaly at T_N is not unreasonable. In addition, the onset of the short-range order at 30 K corresponds to the turning point of the resistivity below which the constant residual resistivity appears (Fig. 5). Therefore, there is a possibility that the residual resistivity may not be due to the usual impurity scattering but related to the short-range magnetic order.

VI. CONCLUSION

The DCNQI-family salts are classified into three groups. The group-I DCNQI salts (which are the salts of Li, Na, K, NH_4 , and Ag) can be regarded as highly one-dimensional conductors, because the path of the conduction electrons is strictly limited in the DCNQI chains due to the poor electron affinity of the counter cations. These salts undergo Peierls transitions between 50 and 100 K,

whereas the electrical conductivities are much affected by the formation of the microdomains. The thermoelectric power is understood by the large-*U* limit of the Hubbard model.

The group-II DCNQI salts, the Cu salts of the halogen-substituted DCNQI, can be treated with the one-dimensional tight-binding band picture with the bandwidth 0.4–0.5 eV at high temperatures, undergoing the Peierls transitions around 200 K, and antiferromagnetic orders of the Cu spins at about 10 K.

The group-III DCNQI salts, namely, (2,5-dimethyl-DCNQI)₂Cu and (2,5-dimethoxy-DCNQI)₂Cu retain metallic conductivity down to the lowest measured temperature. At 5.5 K, a magnetic transition similar to that for the group-II DCNQI salts takes place in (2,5-dimethyl-DCNQI)₂Cu with the metallic conduction retained.

The average charge of Cu has been determined as $\text{Cu}^{1.3+}$ from XPS and the $2k_F$ satellites.⁸ This mixed valency results from the comparable electron affinity of Cu and DCNQI, and enhances the interchain interaction to suppress the Peierls transition in the group-III salts. The Cu^{2+} atoms, in turn, tend to be accompanied by the Jahn-Teller distortion, result in large electron-lattice coupling, and increase the Peierls transition temperatures of the group-II DCNQI salts compared with the group-I DCNQI salts. Thus the mixed-valence Cu does not always suppress, but sometimes enhances, the Peierls instability. In contrast to the group-I DCNQI salts which act as typical one-dimensional conductors, the Cu salts contain, associated with their mixed valency, some intriguing (as-yet-unfamiliar) properties among the conventional organic conductors.

ACKNOWLEDGMENTS

The authors are grateful to Dr. K. Imaeda, Dr. S. Bandow, and Dr. T. Inabe for help in the ESR measurements. The authors would like to thank Dr. T. Enoki for helpful discussion about the magnetic transition, and Dr. J. Kondo (Electrotechnical Laboratory) for propounding the question of the order of Cu^{2+} in (2,5-dimethyl-DCNQI)₂Cu.

¹For a review, see I. F. Shchegolev, *Phys. Status Solidi* **12**, 9 (1972).

²For a recent review, see J. R. Ferraro and J. M. Williams, *Introduction of Synthetic Electrical Conductors* (Academic, New York, 1987).

³H. Akamatu, H. Inokuchi, and Y. Matsunaga, *Nature (London)* **173**, 168 (1954).

⁴L. Brossard, M. Ribault, M. Bousseau, L. Valade, and P. Casoux, *C. R. Acad. Sci. Ser. B* **302**, 205 (1986).

⁵A. Kobayashi, H. Kim, Y. Sasaki, R. Kato, H. Kobayashi, S. Moriyama, Y. Nishio, K. Kajita, and W. Sasaki, *Chem. Lett. (Tokyo)* **1987**, 1819.

⁶A. Aumüller, P. Erk, G. Klebe, S. Hünig, J. U. Schutz, and H.-P. Werner, *Angew. Chem. Int. Ed. Engl.* **25**, 740 (1986).

⁷A. Aumüller and S. Hünig, *Liebigs Ann. Chem.* **1986**, 165.

⁸A. Kobayashi, R. Kato, H. Kobayashi, T. Mori, and H. Inokuchi, *Solid State Commun.* **64**, 45 (1987).

⁹R. Kato, H. Kobayashi, A. Kobayashi, T. Mori, and H. Inokuchi, *Chem. Lett. (Tokyo)* **1987**, 1579.

¹⁰T. Mori, K. Imaeda, R. Kato, A. Kobayashi, H. Kobayashi, and H. Inokuchi, *J. Phys. Soc. Jpn.* **56**, 3429 (1987).

¹¹The Na salts crystallize a monoclinic system, but the essential features of the crystal structures are the same.

¹²R. B. Somoano, A. Gupta, V. Hadek, T. Datta, M. Jones, R. Deck, and A. M. Hermann, *J. Chem. Phys.* **63**, 4970 (1975).

¹³H. Kobayashi and K. Kobayashi, *Bull. Chem. Soc. Jpn.* **50**, 3127 (1977).

¹⁴Since the logarithmic derivative of the resistivity unfortunately shows no definite divergence, the metal-insulator transition temperature T_{M-I} is, somewhat arbitrarily, defined as the

- steep rise of the resistivity. In Ref. 9, the minimum of the resistivity is regarded as T_{M-I} .
- ¹⁵H. Kobayashi, R. Kato, A. Kobayashi, T. Mori, and H. Inokuchi, *Solid State Commun.* **65**, 1351 (1988).
- ¹⁶P. E. Seiden and D. Cabib, *Phys. Rev. B* **13**, 1846 (1976); C. K. Chiang, M. J. Cohen, A. F. Garito, A. J. Heeger, C. M. Mikulski, and A. G. MacDiarmid, *Solid State Commun.* **18**, 1451 (1976).
- ¹⁷P. M. Chaikin, J. F. Kwak, and A. J. Epstein, *Phys. Rev. Lett.* **42**, 1178 (1979).
- ¹⁸J. F. Kwak and G. Beni, *Phys. Rev. B* **13**, 652 (1976).
- ¹⁹P. M. Chaikin and G. Beni, *Phys. Rev. B* **13**, 647 (1976).
- ²⁰P. M. Chaikin, R. L. Greene, S. Etemad, and E. Engler, *Phys. Rev. B* **13**, 1627 (1976).
- ²¹J. B. Torrance, in *Chemistry and Physics of One-Dimensional Metals* Vol. 25 of *Nato Advanced Study Institute, Series B: Physics*, edited by H. J. Keller (Plenum, New York, 1977), p. 161.
- ²²T. Mori, Y. Yokogawa, A. Kobayashi, Y. Sasaki, and H. Kobayashi, *Solid State Commun.* **49**, 249 (1984).
- ²³R. P. Huebener, in *Solid State Physics*, edited by H. Ehrenreich, F. Seitz, and D. Turnbull (Academic, New York, 1972), Vol. 17, p. 63; D. K. C. MacDonald, *Thermoelectricity: An Introduction to the Principles* (Wiley, New York, 1962); R. D. Barnard, *Thermoelectricity in Metals and Alloys* (Taylor and Francis, London, 1972).
- ²⁴R. W. Tsien, C. M. Huggins, and O. H. LeBlanc, Jr., *J. Chem. Phys.* **45**, 4370 (1966).
- ²⁵Y. Tomkiewicz, E. M. Engler, and T. D. Schultz, *Phys. Rev. Lett.* **18**, 456 (1975).
- ²⁶R. J. Elliott, *Phys. Rev.* **96**, 266 (1954).
- ²⁷A. Abragam and B. Bleaney, *Electron Paramagnetic Resonance of Transition Ions* (Clarendon, Oxford, 1970).
- ²⁸The tetrahedral d^9 system is equivalent to the octahedral d^1 system, which is analyzed in pp. 417–426 of Ref. 27. The ground state of the d^9 system is the A level of Fig. 7.21, Table 7.9, and Table 7.10 of Ref. 27.
- ²⁹The calculation was performed for a hypothetical compound, $[\text{Cu}(\text{NH}_3)_4]^{2+}$, where the N atoms are placed on the same positions as the N atoms of 2,5-dimethyl-DCNQI determined by the x-ray crystal structure analysis.⁸ The method of the calculation was the extended Hückel method that was used in Ref. 8.
- ³⁰Table 7.9 of Ref. 27.
- ³¹The splitting of the E_g level is neglected according to the model calculation.
- ³²The same Δ is, in another way, obtained by using Eq. (6) for the E doublet.
- ³³B. N. Figgis, *Introduction to Ligand Field Theory* (Wiley Interscience, New York, 1966).
- ³⁴R. E. Dietz, H. Kamimura, M. D. Sturge, and A. Yariv, *Phys. Rev.* **132**, 1559 (1963).
- ³⁵A. H. Maki and B. R. McGarvey, *J. Chem. Phys.* **29**, 31 (1958).
- ³⁶L. J. de Jongh and A. R. Miedema, *Experiments on Simple Magnetic Model Systems* (Taylor and Francis, London, 1974).
- ³⁷M. de Wit and A. R. Reinberg, *Phys. Rev.* **163**, 261 (1967); A. Hausmann and P. Schreiber, *Solid State Commun.* **7**, 631 (1969).
- ³⁸E. H. Carlson and R. D. Spence, *J. Chem. Phys.* **24**, 471 (1956).
- ³⁹R. H. Taylor, *Adv. Phys.* **24**, 681 (1975).
- ⁴⁰J. B. Torrance, H. J. Pedersen, and K. Bechgaard, *Phys. Rev. Lett.* **49**, 881 (1982).
- ⁴¹N. R. James, S. Legvold, and F. H. Spedding, *Phys. Rev.* **88**, 1092 (1952).